# Semiempirical Calculations of the Electronic Absorption Spectrum of Mitochondrial Aspartate Aminotransferase. 2. The 2-Methylaspartate Complex

**P. A. Clark, J. N. Jansonius, and E. L. Mehler*,†**

*Contribution from the Department of Structural Biology, Biocenter of the University of Basel, Klingelbergstrasse 70, CH-4056 Basel, Switzerland*

*Received April 7, 1993®*

**Abstract:** The electronic transitions of the covalent external aldimine adduct of aspartate aminotransferase with the inhibitor L-2-methylaspartate have been calculated using the semiempirical, all-valence-electron INDO/S method with configuration interaction. The electronic absorption spectra of several protonation states of the system were evaluated and compared with the observed solution spectrum. The model used for the calculation consists of the vitamin $B_6$ cofactor with covalently bound 2-methylaspartate and nine residues from the protein which interact directly or indirectly with the cofactor. The cofactor's pyridine ring is hydrogen bonded to Tyr225, Asn194, and Asp222 and is $\pi$-stacked with the indole ring of Trp140. In addition, Arg292 and Arg386, which are H-bonded to the carboxylate groups of the inhibitor, and His143, Ser139 and one water molecule, which modulate the interaction of Asp222 with the pyridine nitrogen, were also included in the calculations. Transitions were calculated for the two states in which the pyridine nitrogen and Asp222 interact either as a neutral or ion pair. For each of these, the three alternatives considered were the protonated and deprotonated aldimine and the enolimine. Geometries were taken from the X-ray structural data with the H-atom positions determined using the AM1 Hamiltonian or placed at standard bond length from the proton donor. A lognormal functional analysis of the calculated transitions of the six ionization states was carried out to construct a simulated solution spectrum. The $\lambda_{max}$ of the bands resulting from this analysis showed good agreement with the experimental values (rms deviation of 6 nm), and the simulated spectrum exhibited a good fit to the observed spectrum. The fitting strongly suggests that at the pH of 7.5 of the measured solution spectrum, the pyridine nitrogen–Asp222 pair can be present in both the charged and neutral states. The plausibility of this result, which contradicts previous assumptions, is discussed, and electrostatic arguments are presented which support the tenability of this conclusion. The orientations of the transition dipole moments were calculated and compared with observed values.

## Introduction

Over the last several decades intensive research has been carried out on the large family of vitamin $B_6$-dependent enzymes that catalyze a wide variety of reactions in the intermediate metabolism of amino acids. These studies are greatly facilitated by the characteristic chromophoric properties of the common cofactor pyridoxal 5′-phosphate (PLP) and its derivatives. Comparison with the spectral properties of isolated pyridoxal and related molecules in solution and of their reaction products with amino acids has made it possible to identify most of the covalent catalytic intermediates in these reactions.[1] Nonetheless, uncertainties remain in the assignment of certain of the observed spectral bands: One problem is the sensitivity of the wavelength maxima of absorption bands to specific interactions of the chromophore with amino acid residues of the protein active site and, another, the dependence of the cofactor's spectral properties on its ionization state.

Resolution of this uncertainty in band assignment is of particular importance and interest in the case of the covalent external aldimine adduct of aspartate: 2-oxoglutarate aminotransferase (EC 2.6.1.1), commonly referred to as aspartate aminotransferase (AspAT), with the inhibitor L-2-methylaspartate (2-MeAsp). This unproductive analog of a covalent catalytic intermediate was investigated in detail by Fasella and co-workers[2] and has been studied crystallographically for chicken mitochondrial AspAT[3–5] and for pig[6,7] and chicken[8] cytosolic AspAT (see ref 9 for a review) as well as for *E. coli* AspAT.[10,11] The covalent adduct's solution spectrum in the 300–500-nm wavelength region is independent of pH in the range 5–11 and consists of a band with its maximum at about 425 nm and additional overlapping bands with maxima near 320 and 360 nm.[12–15] The 425-nm absorption band has always been attributed to the protonated aldimine form of the covalent adduct, but the origin of the 360-

† Permanent address after Oct. 1, 1993: Department of Physiology & Biophysics, Mt. Sinai School of Medicine, One Gustave L. Levy Place, New York, NY 10029.

® Abstract published in *Advance ACS Abstracts*, October 1, 1993.

(1) *Vitamin $B_6$. Pyridoxal Phosphate*; Dolphin, D., Poulson, R., Avramovich, O. Eds.; John Wiley: New York, 1986.

(2) Fasella, P.; Giartosio, A.; Hammes, G. G. *Biochem.* **1966**, *5*, 197–202.

(3) Jansonius, J. N.; Eichele, G.; Ford, G. C.; Picot, D.; Thaller, C.; Vincent, M. G. In *Transaminases*; Christen, P., Metzler, D. E., Eds.; John Wiley: New York, 1985; pp 110–138.

(4) Picot, D. Ph.D. Dissertation, University of Basel, Switzerland, 1986.

(5) McPhalen, C. A.; Vincent, M. G.; Picot, D.; Jansonius, J. N.; Lesk, A. M.; Chothia, C. *J. Mol. Biol.* **1992**, *227*, 197–213.

(6) Metzler, C. M.; Metzler, D. E.; Martin, D. S.; Newman, R.; Arnone, A.; Rogers, P. *J. Biol. Chem.* **1978**, *253*, 5251–5254.

(7) Arnone, A.; Rogers, P. H.; Hyde, C. C.; Briley, P. D.; Metzler, C. M.; Metzler, D. E. In *Transaminases*; Christen, P., Metzler, D. E., Eds.; John Wiley: New York, 1985; pp 138–155.

(8) Borisov, V. V.; Borisova, S. N.; Kachalova, G. S.; Sosfenov, N. I.; Vainshtein, B. K. In *Transaminases*; Christen, P., Metzler, D. E., Eds.; John Wiley: New York, 1985; pp 155–164.

(9) Jansonius, J. N.; Vincent, M. G. In *Biological Macromolecules and Assemblies*; Jurnak, F. A., McPherson, A., Eds.; John Wiley: New York, 1987; Vol. 3, pp 187–285.

(10) Inoue, K.; Kuramitsu, S.; Okamoto, A.; Hirotsu, K.; Higuchi, T.; Kagamiyama, H. *Biochem.* **1991**, *30*, 7796–7801.

(11) Jaeger, J. Ph.D. Dissertation, University of Basel, Switzerland, 1991.

(12) Rossi, G. L.; Ottonello, S.; Mozzarelli, A.; Tagoni, M.; Martini, F.; Bossa, F.; Fasella, P. In *Protein: Structure, Function and Industrial Applications; Proceedings of the 12th FEBS Meeting*; Hofman, E., Pfeil, W., Aurich, H. Eds.; Pergamon Press: Oxford, 1979; Vol. 52, pp 249–258.

(13) (a) Makarov, V. L.; Kochkina, V. M.; Torchinsky, Yu. M. *FEBS Lett.* **1980**, *114*, 79–82. (b) Makarov, V. L.; Kochkina, V. M.; Torchinsky, Y. M. *Biochim. Biophys. Acta* **1981**, *659*, 219–228.

(14) Eichele, G.; Karabelnik, D.; Halonbrenner, R.; Jansonius, J. N.; Christen, P. *J. Biol. Chem.* **1978**, *253*, 5239–5242.

(15) Hubert, E.; Martinez-Carrion, M. *J. Protein Chem.* **1982**, *1*, 163–175.

0002-7863/93/1515-9789$04.00/0 

nm band is still under debate, being ascribed either to an unprotonated external aldimine[2,9] or to the unprotonated internal PLP-Lys258 aldimine in the Michaelis complex with the inhibitor before covalent bonding occurs.[7,13,16,17] In the crystal structures there is no doubt that the inhibitor is covalently bound to the coenzyme, and since the crystal spectra also display strong absorption in the 360-nm region, the quite intense 360-nm maximum in solution is most likely also due to the external aldimine intermediate.[9]

Experimental studies on model PLP systems in solution have been reported by Heinert and Martell[18] and Metzler *et al.*[19] (See ref 20 for a review of these and related studies.) Heinert and Martell[18] measured the spectra of the aldimine of 3-hydroxypyridine-4-aldehyde with valine in the solid state (KBr pellets) and in dioxane and methanol solutions. At neutral pH they found two tautomeric forms, a protonated aldimine absorbing at 425 nm and an enolimine absorbing at 324 nm. At alkaline pH the unprotonated aldimine absorbed at 361 nm. Protonation of the pyridine N1 of the cofactor was observed to lead in general to a shift of the absorption maxima by only a few nanometers. (See, however, plate III in ref 18b, which shows a shift of 20 nm between the unprotonated aldimines, species IVB and VII.) Metzler *et al.*[19] reported spectral studies on a series of aldimines. From the spectrum of PLP with valine, in both aqueous and methanol solution, they determined a $pK_a$ of 6.8 for the deprotonation of N1. Equilibrium measurements showed the major species to be the protonated aldimine, with the enolimine and the unprotonated aldimine present at low concentration. Resonance Raman studies[21] indicate that N1 is protonated in the 2-MeAsp complex of cAspAT as well as in the model system. One motivation for the present study was to investigate whether the solution spectrum of the AspAT–2-MeAsp adduct can indeed be explained by a mixture of different protonation states of the external aldimine intermediate, which would substantiate the tentative conclusion based on the crystal structure and the crystal spectra.

Semiempirical quantum mechanical methods have been applied in efforts to explain the visible and near ultraviolet spectra of the PLP cofactor in AspAT. Morozov[22] has reviewed Pariser–Parr–Pople $\pi$-electron calculations on various forms of PLP and PMP for comparison with spectra of model systems in solution. H-bonding effects were treated empirically. We recently described the application of the INDO/S all-valence-electron method[23,24] in assigning AspAT spectra.[25] This method was applied to models based on the crystal structures of chicken mAspAT for the unliganded PLP-enzyme at high pH (HPH) and at low pH (LPH) and the pyridoxamine 5′-phosphate form, PMP, including up to seven groups representing residues interacting with the cofactor in the enzyme's active site.[26,27] Electronic absorption spectra, transition dipole moments (TDM), and the

**Scheme I**

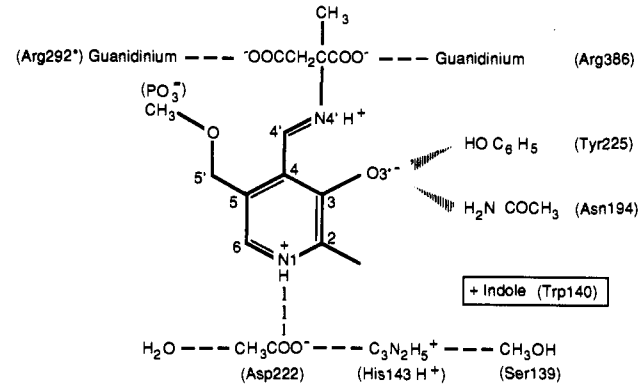


contributions of different protonation states were evaluated for the three enzyme forms. The calculated results were generally in good agreement with experiment.

In the present study the method described in earlier work[25] has been applied to the covalent external aldimine of mAspAT with 2-MeAsp (AMA). The model structures include the seven residues used in the HPH and LPH models, and, in addition, guanidinium cations representing arginine residues Arg386 and Arg292* (the latter from the second subunit) which are H-bonded to the carboxylate groups of 2-MeAsp in the inhibitor complex. These nine residues are shown in Scheme I. Lys258 is modeled by methylamine (not shown). See ref 5 for a stereodiagram.

The spectra of six different protonation states were calculated in order to assist in the assignment of the bands found in the solution spectrum. These states include (a) the protonated external aldimine, (b) its corresponding enolimine with the aldimine N4′ proton transferred to the otherwise ionized 3-hydroxyl group, and (c) the unprotonated external aldimine; in each case either with both N1 and the Asp222 side chain charged (I) or with both neutral (II).

## Methods

**Calculations.** The model complexes were constructed as described previously.[25] Geometries for the C, N, and O atoms used as input to the spectral calculations are taken from the X-ray structure which has been deposited with the Brookhaven Protein Data Bank[28] (code no. 1AMA); the hydrogen positions are optimized using the AM1 method.[29] The spectral calculations are based on the semiempirical self-consistent-field (SCF) INDO method,[30] extended to the prediction of excited states by Ridley, Bacon, and Zerner,[23,24] using the parameters given in Table I of ref 25. Between 300 and 350 configurations were included in the CI calculations with an excitation energy cutoff of about 6.5 eV.

**Solution Spectra.** Absorption spectra of AMA in sodium phosphate buffered solution at pH 7.5 with a protein concentration of 0.76 mg/mL were recorded on a Uvikon 860 spectrophotometer (Kontron Instruments). Spectra were deconvoluted with lognormal functions.[31]

**Simulated Spectra.** Calculated wavelengths and intensities have been used as parameters in lognormal functions to simulate spectra[25] for comparison with the observed solution spectra.

## Results and Discussion

**Geometry.** In contrast to the forms of mAspAT studied in ref 25, the AM1 method predicts the protonated external aldimine

(16) Torchinsky, Yu. M. In *Vitamin $B_6$. Pyridoxal Phosphate*; Dolphin, D., Poulson, R., Avramovich, O., Eds.; John Wiley: New York, 1986; Part A, pp 131–180.
(17) Metzler, C. M.; Mitra, J.; Metzler, D. E.; Makinen, M. W.; Hyde, C. C.; Rogers, P. H.; Arnone, A. *J. Mol. Biol.* **1988**, *203*, 197–220.
(18) (a) Heinert, D.; Martell, A. E. *J. Am. Chem. Soc.* **1963**, *85*, 183–188; (b) Heinert and Martell *J. Am. Chem. Soc.* **1963**, *85*, 188–193.
(19) Metzler, C. M.; Cahill, A.; Metzler, D. E. *J. Am. Chem. Soc.* **1980**, *102*, 6075–6082.
(20) Kallen, R. G.; Korpela, T.; Martell, A. E.; Matsushima, Y.; Metzler, C. M.; Metzler, D. E.; Morosov, Y. V.; Ralston, I. M.; Savin, F. A.; Torchinsky, Y. M.; Ueno, H. In *Transaminases*; Christen, P.; Metzler, D. E., Eds.; John Wiley: New York, 1985; pp 37–108.
(21) Benecky, M. J.; Copeland, R. A.; Rava, R. P.; Feldhaus, R.; Scott, R. D.; Metzler, C. M.; Metzler, D. E.; Spiro, T. G. *J. Biol. Chem.* **1985**, *260*, 11671–11678.
(22) Morozov, V. Y. In *Vitamin $B_6$. Pyridoxal Phosphate*; Dolphin, D., Poulson, R., Avramovich, O., Eds.; John Wiley: New York, 1986; Part A, pp 131–180.
(23) Ridley, J.; Zerner, M. C. *Theor. Chim. Acta* **1973**, *32*, 111–134.
(24) Bacon, A. D.; Zerner, M. C. *Theor. Chim. Acta* **1979**, *53*, 21–54.
(25) Clark, P. A.; Jansonius, J. N.; Mehler, E. L. *J. Am. Chem. Soc.* **1993**, *115*, 1894–1902.
(26) Kirsch, J. F.; Eichele, G.; Ford, G. C.; Vincent, M. G.; Jansonius, J. N.; Gehring, H.; Christen, P. *J. Mol. Biol.* **1984**, *174*, 497–525.
(27) McPhalen, C. A.; Vincent, M. G.; Jansonius, J. N. *J. Mol. Biol.* **1992**, *225*, 495–517.
(28) Bernstein, F. C.; Koetzle, T. F.; Williams, G. J. B.; Meyer, E. J., Jr.; Brice, M. D.; Rogers, J. R.; Kennard, O.; Shimanouchi, T.; Tasumi, M. *J. Mol. Biol.* **1977**, *112*, 535–542.
(29) (a) Dewar, M. J. S.; Zoebisch, E. G.; Healy, E. F.; Stewart, J. J. P. *J. Amer. Chem. Soc.* **1985**, *107*, 3902–3909. (b) AMPAC: Austin Method 1 (QCPE 506); version 1.0. Dewar Research Group and J. J. P. Stewart *QCPE Bull.* **1986**, *6*, 24.
(30) Pople, J. A.; Beveridge, D. L. *Approximate Molecular Orbital Methods*; McGraw-Hill: New York, 1970.
(31) Siano, D. B.; Metzler, D. E. *J. Chem. Phys.* **1969**, *51*, 1856–1861.

**Table I.** Calculated Wavelengths (λ), Intensities (ε), and Directions of the Transition Dipole Moments (ω)[a] for Different Protonation States of AMA

| AMA species | calculated | | | simulated | | | $\lambda_{max}$, obs (nm) | |
|---|---|---|---|---|---|---|---|---|
| | λ (nm) | ε ($M^{-1}$ $cm^{-1}$) | ω (deg) | $\lambda_{max}$ (nm) | ε ($M^{-1}$ $cm^{-1}$) | ω (deg) | enzyme (soln) | model PLP |
| I. N1, Asp222 charged | | | | | | | | |
| a. N4′ protonated | 448.6 | 9191 | 38 | 448 | 8530 | 43 | 445,[b] 426,[c] 427[d] | 415,[e] 417[f] |
| | 409.6 | 1267 | 59 | | | | | |
| | 371.8 | 999 | 17 | ~355 | ~2700 | −15 | 359,[b,c] 361[d] | |
| | 359.0 | 272 | −57 | | | | | |
| | 344.9 | 1949 | −23 | | | | | |
| | 324.8 | 3050 | 48 | 329 | 4260 | 48 | 319[b,d] | 320–330[e] |
| b. O3′ protonated | 476.6 | 154 | 86 | | | | | |
| | 365.4 | 333 | 31 | 356 | 9900 | 18 | 359,[b,c] 361[d] | 330,[e] 327[g] |
| | 362.2 | 4070 | 32 | | | | | |
| | 358.4 | 5924 | −23 | | | | | |
| | 340.9 | 81 | 82 | | | | | |
| | 337.5 | 1460 | 74 | | | | | |
| | 305.6 | 699 | 15 | 303 | 7300 | 15 | | |
| | 299.2 | 2244 | 12 | | | | | |
| | 297.7 | 3212 | 18 | | | | | |
| c. N4′, O3′ not protonated | 395.5 | 13024 | 31 | 396 | 12020 | 31 | | 347,[e] 386,[f] 380[g] |
| | 332.3 | 485 | −32 | | | | | |
| | 316.4 | 1136 | 54 | 312 | 3200 | 32 | | |
| | 312.3 | 977 | −29 | | | | | |
| | 309.4 | 558 | 69 | | | | | |
| | 301.3 | 200 | −32 | | | | | |
| | 301.1 | 463 | 85 | | | | | |
| II. N1, Asp222 neutral | | | | | | | | |
| a. N4′ protonated | 437.7 | 8047 | 31 | 430 | 8827 | 36 | 425,[b] 426,[c] 427[d] | 425,[e,g] 416[f] |
| | 414.4 | 2467 | 46 | | | | | 350[d] |
| | 328.1 | 178 | 66 | 301 | 5493 | 3 | 319[b,d] | 325[e] |
| | 312.8 | 1854 | −15 | | | | | |
| | 304.9 | 2326 | 77 | | | | | |
| | 295.4 | 2647 | −46 | | | | | |
| b. O3′ protonated | 429.6 | 236 | −66 | | | | | |
| | 329.9 | 473 | 84 | 308 | 8725 | 5 | 319[b,d] | 330,[e] 322,[f] 324[g] |
| | 323.4 | 6182 | 26 | | | | | |
| | 301.9 | 3882 | −25 | | | | | |
| | 300.6 | 1345 | −21 | | | | | |
| c. N4′, O3′ not protonated | 383.1 | 3906 | 14 | 360 | 9736 | 23 | 359,[b,c] 361[d] | 345,[e] 361[g] |
| | 358.4 | 7842 | 30 | | | | | |
| | 354.6 | 197 | ~0 | | | | | |
| | 343.4 | 622 | 33 | | | | | |
| | 330.0 | 143 | −4 | | | | | |
| | 324.9 | 280 | −76 | | | | | |
| | 319.8 | 1612 | 62 | | | | | |

[a] ω is given with respect to the N1–C4 axis of the PLP pyridine ring. The wavelength maxima of the spectra simulated using lognormal functions are correlated with observed values for the enzyme in solution and for model PLP systems. [b] This work; parameters for bandwidth and skewness used in the simulation are given in Table III. [c] Reference 20. Mitochondrial AspAT; pH 8.3. [d] Reference 20. Cytosolic AspAT; pH 7.0. [e] Reference 19. [f] Reference 34. [g] Reference 18.

with both N1 and Asp222 neutral (species IIa in Table I) to be appreciably more stable than the species in which these groups are charged (species Ia in Table I). The calculated heats of formation differ by 47 kcal/mol for the protonated aldimines and 48 kcal/mol for the enolimines (species Ib and IIb in Table I). Recent X-ray analysis shows that H-bonding distances between N1 and Asp222 are maintained on formation of the external aldimine, and current proposals postulate that N1 is protonated at all steps in the transaldimination reaction mechanism.[9,21,26,32] Only for species IIa could all the hydrogen atom positions be fully optimized; using this structure, those for the other protonation states were generated by placing the proton bonded to N1, Asp222, O3′, or N4′ (see Scheme I) at a distance of 1.0 Å from its binding partner.

**Spectra.** Consistent with the most recent proposals for the enzyme reaction mechanism, we first calculated the absorption spectrum of AMA assuming N1 protonated and Asp222 charged (species Ia, Table I). The simulated spectrum gave an absorption maximum of 448 nm, appreciably to the red of the $\lambda_{max}$ at 427 nm observed in both solution and crystal spectra.[20] In contrast, calculations using the AM1 optimized proton position with N1 and Asp222 neutral, species IIa, gave a simulated spectrum with $\lambda_{max}$ at 430 nm. For the enolimine Ib (Table I) the simulated $\lambda_{max}$ is 356 nm, compared to the observed band maximum at 359 nm; that for the enolimine IIb is 308 nm, at shorter wavelength than the observed value of 319 nm but within acceptable error limits. The predicted maximum for the unprotonated external aldimine (IIc) is at 360 nm which is also in agreement with the observed band at 359 nm. The external aldimine Ic has a calculated absorption maximum at 396 nm (see Table I).

The band observed at 427 nm for AMA is adequately described by a single lognormal function, with the exception of the long wavelength tail which exhibits a larger deviation from the observed spectrum (see, for example, Figure 2.17 of ref 20). We find that the predicted $\lambda_{max}$ of species IIa provides an adequate assignment of this band, but again with the larger deviation in the long wavelength region. Although it has always been assumed that this band is due to species Ia, our calculations suggest it is due to species IIa. Given that both species are present, it is reasonable to use two lognormal functions to represent the 427-nm band of the solution spectrum. These are designated bands 1 and 1′ in Table II. It must be emphasized that the parameters given in Table II for the two functions fitted to band 1 of the observed solution spectrum in no way imply a quantitative measure of the actual equilibrium concentrations of the species existing in solution, because the fitting of the long wavelength band of the

**Table II.** Parameters Used in Fitting Lognormal Functions to the Solution Spectrum of AMA

| band | $\lambda_0$ (nm) | $\epsilon_0$ ($M^{-1}$ $cm^{-1}$) | width ($cm^{-1}$) | $\rho$ |
|---|---|---|---|---|
| 1′ | 445 | 1100 | 3800 | 1.6 |
| 1 | 425 | 3000 | 3800 | 1.6 |
| 2 | 359 | 3500 | 4800 | 1.7 |
| 3 | 319 | 2500 | 4800 | 1.6 |
| 4 | 280 | 22500 | 5000 | 1.5 |

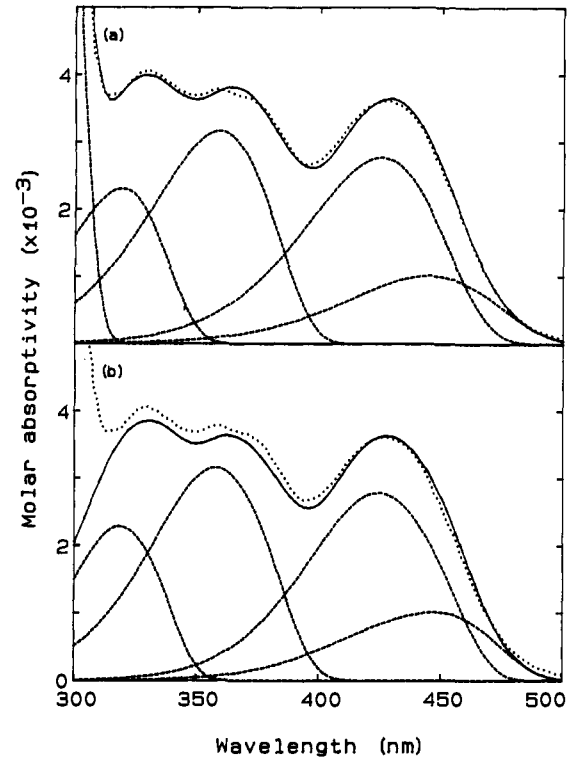


**Figure 1.** (a) Lognormal distribution functions (– –) and their sum (—) fit to the solution spectrum (· · ·) of AMA using the parameters in Table II. (b) Calculated spectrum of AMA (—) as a sum of simulated bands (– –) composed of the lognormal functions defined by the predicted $\lambda_0$ and other parameters given in Table III, compared with the solution spectrum (· · ·).

solution spectrum with two lognormal functions does not permit their unique definition. Due to extensive overlapping of the two assumed functions, both the $\lambda_0$'s and the $\epsilon_0$'s can be varied over a rather large range of values. For example, it would be possible, by shifting both $\lambda_0$'s to shorter wavelength, to find an $\epsilon_0$ for Ia larger than that for IIa, implying a change in their relative concentrations in solution but nevertheless providing an adequate fit to the 427-nm band of the observed spectrum. Moreover, the calculated wavelengths cannot be expected to be sufficiently accurate to permit their use in defining a unique $\lambda_0$ for the lognormal fitting of the solution spectrum, although in the present work they have been so used, as a first approximation.

A simulated solution spectrum obtained by combining bands 1 and 1′ with the remaining bands given in Table II is shown in Figure 1a. It is clear that the fit is quite good and reproduces the long wavelength tail of the spectrum better than an alternative fitting with only one lognormal function for the 427-nm band. An apparent shoulder on the 360-nm band could not be fitted with an additional function and may be due to vibrational fine structure.[31,33]

(31) Arnone, A.; Christen, P.; Jansonius, J. N.; Metzler, D. E. In *Transaminases*; Christen, P., Metzler, D. E., Eds.; John Wiley: New York, 1985; pp 326–357.
(32) Metzler, D. E., Harris, C. M., Johnson, R. I., Siano, D. B., Thomson, J. A. *Biochem.* **1973**, *12*, 5377–5392.

**Table III.** Parameters Used in Fitting the Calculated Transitions to Lognormal Functions Found for the Solution Spectrum of AMA

| band | species | $\lambda_0$ (nm) | $\lambda_0 - \lambda_{calc}$ | $\epsilon_0$ ($M^{-1}$ $cm^{-1}$) | $\frac{\epsilon_0}{\epsilon_{calc}}$ | width ($cm^{-1}$) | $\rho$ |
|---|---|---|---|---|---|---|---|
| 1′ | Ia | 449 | 0 | 1093 | .12 | 3200 | 1.6 |
| | | 410 | 0 | 151 | .12 | 3200 | 1.6 |
| 1 | IIa | 432 | –6 | 2567 | .32 | 3250 | 1.6 |
| | | 408 | –6 | 787 | .32 | 3250 | 1.6 |
| 2 | Ia | 373 | 1 | 119 | .12 | 4250 | 1.7 |
| | | 360 | 1 | 32 | .12 | 4250 | 1.7 |
| | | 346 | 1 | 232 | .12 | 4250 | 1.7 |
| | with Ib | 368 | 3 | 96 | .29 | 4250 | 1.7 |
| | | 365 | 3 | 1177 | .29 | 4250 | 1.7 |
| | | 361 | 3 | 1714 | .29 | 4250 | 1.7 |
| | | 341 | 3 | 422 | .29 | 4250 | 1.7 |
| | or with IIc | 383 | 0 | 1172 | .30 | 4250 | 1.9 |
| | | 358 | 0 | 2353 | .30 | 4250 | 1.9 |
| | | 355 | 0 | 59 | .30 | 4250 | 1.9 |
| | | 343 | 0 | 187 | .30 | 4250 | 1.9 |
| 3 | Ia | 325 | 0 | 363 | .12 | 4000 | 1.6 |
| | IIa | 322 | –6 | 44 | .32 | 4000 | 1.6 |
| | | 307 | –6 | 464 | .32 | 4000 | 1.6 |
| | IIb | 330 | 0 | 118 | .26 | 4000 | 1.6 |
| | | 323 | 0 | 1546 | .26 | 4000 | 1.6 |

The results of fitting the calculated transitions of Table I to the solution spectrum as described in ref 25 are given in Table III. For some species the predicted wavelengths have been shifted slightly to improve the agreement with experiment ($\lambda_0 - \lambda_{calc}$ in Table III), but these shifts are small, at most ±6 nm. A scaling factor for the calculated absorption coefficients is given by $\epsilon_0/\epsilon_{calc}$. It should be noted that for a given species the same shifting or scaling has been applied to all calculated transitions given in Table I. For those which display multiple maxima in their simulated spectra, as indicated in Table I, sets of transitions have been fit to the corresponding bands of the solution spectrum which lie in the same wavelength region. Thus, for example, the first two transitions listed in Table I for species Ia are fit to band 1′, the next three are fit to band 2, and the last is fit to band 3. Transitions in Table I with $\lambda < 310$ nm were not included in constructing the curve for comparison with the solution spectrum.

It is not possible, on the basis of the calculations reported here, to determine whether band 2 of the solution spectrum is due to the enolimine Ib or the unprotonated external aldimine IIc, since both have a predicted $\lambda_{max}$ of 360 nm (see Table I). Both may exist in solution, but there is no way to estimate their relative concentrations. Thus in Table III, parameters for fitting the calculated spectrum of either one or the other of these to band 2 of the solution spectrum are included. The simulated band combining the parameters of species Ia and Ib agrees better with the resolved band shown in Figure 1a than the simulated band constructed from Ia and IIc, since the longer wavelength transition predicted at 383 nm for the latter gives too strong an absorbance in this region. In addition, a good fit of the calculated spectrum for species IIc requires the assumption of a rather large value for the skewness parameter.

For each of the four bands in Table III, but including species Ib rather than IIc for band 2, the sum of the lognormal functions for the transitions listed is shown in Figure 1b. That is, each curve in Figure 1b constructed from the calculated transitions given in Table III corresponds to a fitted band of the solution spectrum in Figure 1a. The sum of the four simulated bands is also shown in Figure 1b, which demonstrates the good agreement with the experimental spectrum.

Transitions calculated for species Ic have not been included in Table III or in Figure 1b, because any contribution to the observed spectrum at the predicted $\lambda_{max}$ of about 400 nm would necessarily be very small, as shown by the already good fit in Figure 1a with no band assumed in this region. Any attempt to include an additional band would thus be very speculative. Transitions for

the species with both N4′ and O3′ protonated, which would only occur at very low pH, were not calculated.

For the two protonated aldimines, Ia and IIa, the dominant transition at longer λ is due to the PLP $\pi \rightarrow \pi^*$ excitation, which has essentially the same energy in the two species. The differences in the calculated λ's arise from the relative extent of mixing of these $\pi \rightarrow \pi^*$ with $n \rightarrow \pi^*$ excitations and from the nature of the lone pair orbitals involved. In Ia the $n_{O3'} \rightarrow \pi^*$ excitation is appreciably lower in energy than excitations arising from lone pair orbitals of the 2-methylaspartate $COO^-$ groups, $n_{ama}$, whereas in IIa the relative excitation energies are reversed. This is most likely an effect of the net charges at the PLP pyridine ring atoms, in particular O3′, which change with the transfer of the proton from N1 to Asp222. In IIa $n_{O3'}$ mixes strongly with both $n_{N1}$ and $n_{ama}$. The blue shift of 18 nm predicted for IIa relative to Ia is of interest since solution spectra of model PLP systems indicate a maximum shift of 4 nm on deprotonation of N1.[18] The larger shift calculated here for model enzyme systems is due to the transfer of the proton from N1 to Asp222 but leaving N1 H-bonded to this now-neutral residue. This has no counterpart in the model PLP systems.[18,19] As discussed earlier,[25] partial neutralization of the −1 charge on Asp222 by inclusion in the model of charged His139 shifts the predicted λ for the LPH form of the internal aldimine by about 10 nm to shorter wavelength. Complete neutralization of the −1 charge on Asp222 by transfer of the proton from N1 could then be expected to cause a larger blue shift.

The MOs of the enolimines Ib and IIb have undergone some rearrangement relative to the ordering found in the protonated aldimines, the $n_{ama}$ MOs now being at higher energy than the two $\pi$ MOs that are the HOMO and HOMO-1 in Ia and IIa. In both enolimines the predicted transitions are a mixture of $\pi \rightarrow \pi^*$ and $n \rightarrow \pi^*$ excitations, where the former are of higher energy than the corresponding excitations of Ia and IIa. In Ib these $\pi$ orbitals are predominantly tryptophan MOs, while in IIb there is mixing of PLP and tryptophan MOs. The lone pair orbitals are predominantly $n_{ama}$. The MOs which contain contributions from $n_{N4'}$ lie at lower energies. While excitations from these MOs form a transition at long wavelength (477 and 430 nm, respectively, for Ib and IIb), they are of negligible intensity.

The predicted $\lambda_{max}$ values for the unprotonated external aldimines Ic and IIc are in reasonably good agreement with the values reported by Karube *et al.*[34] and Heinert and Martell[18] but differ appreciably from those of Metzler *et al.*[19] The species Ic and IIc could correspond, for example, to the AMA enzyme form in which the proton is transferred from the aldimine N to the $N^{\epsilon}$ of the Lys258 residue.[2] The predicted spectrum of Ic originates in excitations from the two highest occupied MOs, which are combinations of the PLP $\pi$ with lone pair orbitals of N4′ and O3′. The predominant excitations of species IIc are PLP $\pi$ to tryptophan $\pi^*$ and to an MO consisting of a combination of PLP and tryptophan $\pi^*$.

**Transition Dipole Moments.** Table I includes the predicted orientation angles ω for the TDMs of the various absorption bands in the simulated spectra for the different protonation states of AMA considered. For the protonated external aldimine the results are 43° for Ia (448 nm) and 36° for IIa (430 nm). Experimentally, no unequivocal result has been obtained for the 427-nm band in mAspAT, since two of the four equivalent solutions obtained in the orthorhombic crystals are compatible with the X-ray structure and give values of 26° and 48°, respectively.[4] For orthorhombic crystals of pig cAspAT complexed with 2-methylaspartate Metzler *et al.*[17] found an ω-value of 27° for the 428-nm absorption band which is in excellent agreement with the alternative value of 26° for chicken mAspAT. The issue remains open to further study.

For the 360-nm band of the crystalline 2-methylaspartate complex of mAspAT linear dichroism data are not accurate. Tentative TDM orientations are most compatible with the external aldimine but do not exclude the internal aldimine with Lys258 as the absorbing species;[4] values for ω were not given. Metzler *et al.*[17] reported the values ω = 6° or 11° for the 368-nm band of the pig cAspAT complex. The present computations for the mAspAT complex gave the values 18° (Ib) and 23° (IIc), rather higher than the experimental values of Metzler *et al.*,[17] but much smaller than the experimental ω-value of about 47° for the 358-nm band of the unprotonated internal aldimine of mAspAT[4] (see ref 25).

## Conclusions

The novel result of the work reported here is the suggestion that both forms I and II of the covalent external aldimine of mAspAT with 2-MeAsp can be present in solution in appreciable concentrations. This differs from the usual assumption that only the form $N1H^+ \cdots Asp222^-$ is present in this system. Given the usual caveats concerning the interpretation of results obtained by semiempirical methods, it is of interest to consider other arguments which support the conclusion that both protonation states can be present and that both can contribute to the observed spectrum.

The $pK_a$ of N1 in mAspAT has not, to the best of our knowledge, been determined, but its $pK_a$ in the PLP-valine aldimine in aqueous solution[19] is 6.8 which means that at a pH of 7.5 about 80% of the coenzyme is deprotonated. In the enzyme the influence of Asp222 will certainly be to increase the $pK_a$. Preliminary calculations of the electrostatic potential (ESP) at N1 of various forms of AspAT by methods described elsewhere[35,36] suggest that without the presence of Asp222, the ESP of the protein is small but shifts the $pK_a$ to slightly lower values. The negatively charged carboxylate group of Asp222 can increase the $pK_a$ of N1 by roughly 2–5 units. Moreover, for the observed separations, very small changes have a large effect on the ESP at N1, i.e., an increase in distance between N1 and the $COO^-$ group from 3.3 to 3.6 Å, could decrease the $pK_a$ of N1 by more than one unit. It is clear therefore that the operative electrostatic interactions allow for a range of $pK$ values for different forms of AspAT. For situations where the interactions increase the $pK$ of N1 by only about 1–3 units, both species I and II will be present in solution at a pH of 7.5. Furthermore, the absolute concentrations of the two forms are rather sensitive to small structural or dynamical changes in the system.

The present study provides insight into the nature of the electronic absorption spectrum of the complex of L-2-methylaspartate with aspartate aminotransferase. The 320-nm band, which has been included in deconvolutions of experimental spectra although a maximum is not always observed,[20] can be explained on the basis of protonic shifts within the external aldimine. The calculations reported here strongly support the interpretation of the 360-nm band as arising from one or more protonation states of the covalent external aldimine structure, rather than an additionally present fraction of unprotonated internal aldimine.

**Acknowledgment.** The authors thank Ursula Sauder for providing the solution spectra, Margrit Jaeggi for help in preparing the diagrams, and the staff of the University of Basel's Computing Center for assistance in running the programs and for technical support. The authors gratefully acknowledge support by Swiss National Science Foundation Grants 31-26261.89 (E.L.M.) and 31-25713.88 (J.N.J.).

(34) Karube, Y.; Ono, Y.; Matsuhima, Y.; Uedo, Y. *Chem. Pharm. Bull.* **1978**, *26*, 2642–2648.
(35) Mehler, E. L.; Eichele, G. *Biochem.* **1984**, *23*, 3887–3891.
(36) Mehler, E. L.; Solmajer, T. *Protein Eng.* **1991**, *4*, 903–910.